

# Kinetic Lattice Group Models: Structure and Numerics

Hans Babovsky

*Institute of Mathematics, Ilmenau University of Technology, Weimarer Str. 25, D-98693 Ilmenau, Germany*

**Abstract.** We investigate properties of a previously proposed discrete kinetic system for the numerical simulation of gas flows on the basis of the Boltzmann equation. On one hand, these models are well-suited for qualitative and quantitative studies in a variety of situations. On the other hand, it is necessary to know about certain features of such schemes. We discuss limitations as well as extensions of the Lattice Group Model.

**Keywords:** Boltzmann equation, numerics, discrete velocity model

**PACS:** 47.45.-n, 02.60.-x, 47.40.-x; **MSC:** 82C40, 76P05

## LATTICE GROUP MODELS

In [1] we have introduced a discrete kinetic model (*Lattice Group Model*, LGM) based on the automorphism group of an integer lattice and have presented first numerical results. The main intention behind the derivation of these systems was to find a construction replacing the inner integral of the Boltzmann collision operator (which is the integration over all possible outcomes of a two-particle collision) with an appropriate sum. The theoretical framework has meanwhile been worked out and published in [2], including a detailed discrete theory along the lines of classical kinetic theory. Here, we discuss the LGM on the most convenient lattice for a discretized 3D velocity space.

The so-called *fcc*-lattice (*face centered cubic* lattice, see [3]) is defined as

$$\mathcal{V} = \{(k, l, m) \in \mathbf{Z}^3 : k + l + m \text{ even}\} \quad (1)$$

and represents the discretized velocity space. The superset  $\mathcal{C} = \mathbf{Z}^3$  represents the set of all center points between colliding particles. In the LGM, for any pair  $(c, v) \in \mathcal{C} \times \mathcal{V}$ , the pair  $(c + (v - c), c - (v - c))$  lies in  $\mathcal{V} \times \mathcal{V}$  and represents a velocity pair undergoing collisions. Denote by  $\mathcal{O}$  the orthonormal group of  $\mathcal{V}$  resp.  $\mathcal{C}$  i.e. the set of all reflections and rotations around zero leaving  $\mathcal{V}$  resp.  $\mathcal{C}$  invariant.  $\mathcal{O}$  contains 48 elements. The discrete homogeneous Boltzmann equation reads

$$\partial_t f(v) = \sum_{c \in \mathcal{C}} \sum_{o \in \mathcal{O}} \gamma_o [f(c + o(v - c))f(c - o(v - c)) - f(v)f(c - (v - c))] =: J[f](v). \quad (2)$$

The weak formulation of  $J[f]$  is

$$\langle J[f], \Phi \rangle = \sum_{c \in \mathcal{C}} \sum_w \sum_{o \in \mathcal{O}} \gamma_o f(c + w)f(c - w) \cdot [\Phi(c + ow) - \Phi(c + w)], \quad (3)$$

where  $\Phi$  is an arbitrary test function on  $\mathcal{V}$  (with compact support), and  $\langle \cdot, \cdot \rangle$  is the usual scalar product in  $\mathbb{R}^{\mathcal{V}}$ . The second sum extends over all  $w = v - c \in \mathcal{C}$  such that  $c + w \in \mathcal{V}$ .

*Finite* kinetic models are obtained replacing  $\mathcal{V}$  with its intersection with the ball  $B_R(0)$  around zero with radius  $R$ ,

$$\mathcal{V}_R = \mathcal{V} \cap B_R(0). \quad (4)$$

In this case the first sum in (2) is restricted to all those  $c \in \mathcal{C}$  for which the discrete sphere

$$S_{c,v} = c + \mathcal{O}(v - c) \subset \mathcal{V} \quad (5)$$

is contained in  $\mathcal{V}_R$ . For some integer values  $R^2$ , Table 1 contains the sizes of  $\mathcal{V}_R$  and the numbers  $|S_R|$  of discrete spheres contained in  $\mathcal{V}_R$ . (These latter numbers correspond to the numerical effort to calculate the collision operator.) The size of choice in numerical calculations depends mainly on the Knudsen numbers  $Kn$ . For  $Kn \ll 1$ ,  $R^2 = 6$  might be a good choice. For larger Knudsen numbers, larger systems have to be chosen. We are going to discuss this in the following.

**TABLE 1.** Size of velocity space

$R^2$	4	6	10	16	20	30
$ \mathcal{V}_R $	19	43	79	141	201	369
$ S_R $	8	23	85	212	421	1194

## SCALING

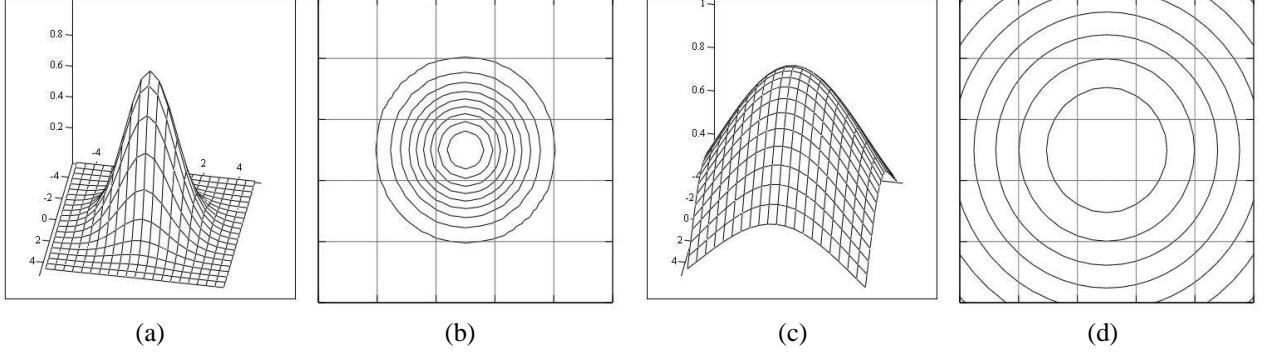


**FIGURE 1.** Maxwellian on finite grid, (a), (b)  $T$  low; (c), (d)  $T$  high.

An LGM with  $|\mathcal{V}_R|$  velocities contains integer velocities up to the limiting radius  $R$ . If we want to represent Maxwellians  $\exp(-|v|^2/2\xi)$  with varying values of  $\xi$  on the finite grid we encounter two types of errors. Figure 1 illustrates this (with a square cut of the grid rather than a circular one). The *discretization error*  $E_{disc}$  decays with increasing  $\xi$  and vanishes for  $\xi \rightarrow \infty$  since the variations of the Maxwellians between neighboring grid points become small. On the contrary, the *truncation error*  $E_{trun}$  which is due to the finiteness of  $R$ , increases. There is an optimal value of  $\xi$  for which the sum of the errors becomes minimal. This situation was tested in the heat layer problem described in [4]. We considered an Argon gas between parallel walls with temperatures of 223.15K and 323.15K at the Knudsen number  $Kn = 0.027$ . The scaling problem consisted in choosing an appropriate value  $\xi$  representing the Maxwellian for the mean temperature  $T_m = 273.15K$ ,

$$\left(\frac{m}{2\pi k T_m}\right)^{3/2} n \exp\left(-\frac{m|v|^2}{2k T_m}\right) \leftrightarrow c \cdot \exp(-|v|^2/2\xi).$$

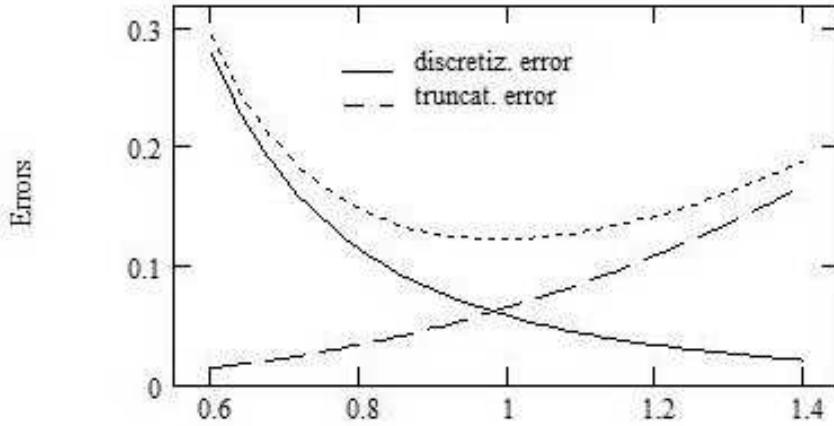


**FIGURE 2.** Discretization and truncation errors.

For the simulation we used the 201-velocity model ( $R^2 = 20$ ). As an error indicator we measured the heat flux  $q$ . It turned out that the errors can with high precision be described as

$$E_{disc} = \alpha_1 \cdot \xi^{-3} + \alpha_2 \cdot \xi^{-6}, \quad E_{trun} = \beta_1 \cdot \xi^3 + \beta_2 \cdot \xi^6.$$

Figure 2 shows the relative errors.  $|E_{disc}| + |E_{trun}|$  takes its minimum at some value  $\xi \approx 1$  with a relative error of approximately 12%. Since LGM calculations are free of fluctuations, this error can be efficiently reduced via interpolation techniques.

### SYMMETRIES, ROTATIONAL FLOWS

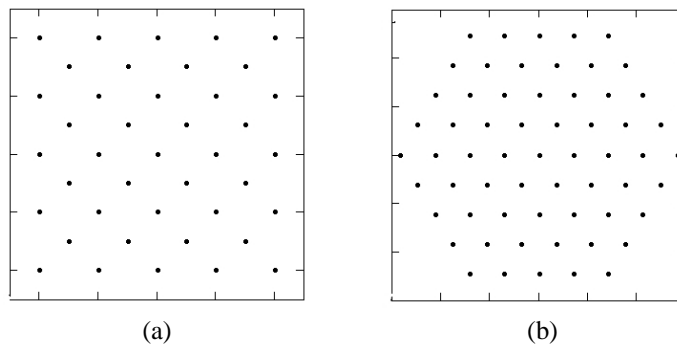


**FIGURE 3.** Plane  $v_z = 0$ , (a) cart., (b) pile.

The fcc model exhibits different rotational symmetries depending on the rotation axis. E.g. there is a  $90^\circ$  rotational symmetry when rotating around the  $z$ -axis and a  $120^\circ$  symmetry (resp. a  $60^\circ$  symmetry in simplified cases) rotating around the axis  $(1, 1, 1)^T$ . We call the velocity space as given in (1) the *cartesian arrangement*. If we transform the velocity space in such a way that the axis  $(1, 1, 1)^T$  becomes the  $z$ -axis, the velocity points are the same as the set of center and contact points of the densest sphere packing of a pile of fruit. This velocity set is called the *pile arrangement*. Figure 3 shows the cuts of the velocity sets with the plane  $v_z = 0$  in the cartesian (a) and the pile (b) arrangement. The choice of the arrangement may be important since the  $90^\circ$  symmetry of the velocity space may produce artefacts when coupled with  $90^\circ$  angles in position space. We demonstrate this in the following example.

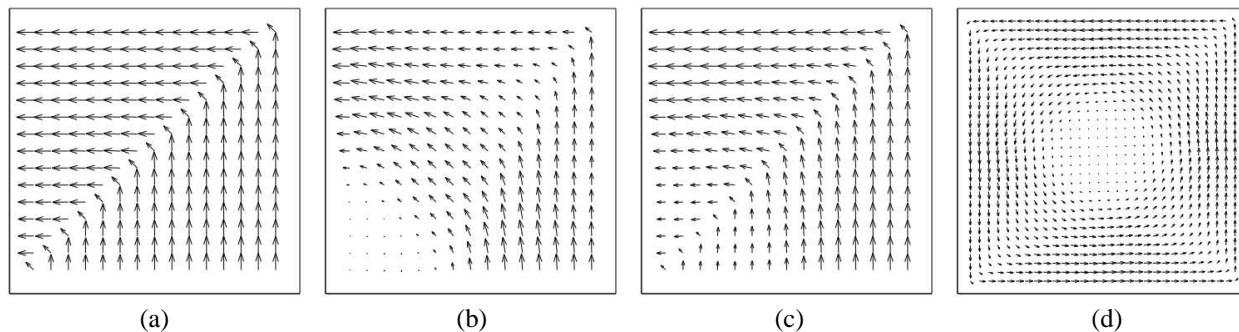


**FIGURE 4.** Boundary driven flow, (a)  $|\mathcal{V}|_R = 43$ , cart., (b)  $|\mathcal{V}|_R = 43$ , pile, (c)  $|\mathcal{V}|_R = 201$ , cart., (d)  $|\mathcal{V}|_R = 201$ , pile.

Consider a spatially 2D flow in a quadratic box with boundaries which impose a momentum in tangential direction (like moving boundaries) in order to generate a rotational flow. In the cartesian arrangement, small systems show the strange behaviour of almost constant axiparallel flow with sharp discontinuities in the diagonals. The upper right quarter of the flow of a 43-velocity model is shown in Fig. 4 (a). The discontinuities in the diagonals are only slightly smoothed when choosing larger models (see Fig. 4 (c) for the 201-velocity model). When applying the pile arrangement, the flow in the interior approaches a rotational flow. In Fig. 4 (b), the flow of the 43-velocity system displays  $90^\circ$  symmetry close to the boundaries forced by the wall interaction. Close to the center, the flow approaches a hexagonal symmetry. Figure 4 (d) shows the flow of the 201-velocity system in the pile arrangement which exhibits a good approximation of a rotational flow in the center.

Rotational flows in  $90^\circ$  spatial arrangements occur in the case of a Knudsen pump in the setting described in [5]. This concerns a plane channel with periodically arranged rectangular ditches. The wall temperature profile is continuous and decreases (resp. increases) linearly inside (resp. outside) the ditches. Temperature gradients at moderate to large Knudsen numbers induce flows in direction of the gradient (this is the so-called *thermal creep flow*). In the above arrangement we get a one-sided flow through the channel, an effect called *Knudsen pump*. The setting in [5] considers temperature variations from a minimum  $T_0$  to the maximum  $3T_0$ . Due to the large temperature variations, the system used for the numerical simulation should not be too small. We applied the 201-velocity model in the pile arrangement. Figure 5 (a) shows the temperature isolines at a Knudsen number  $Kn = 0.16$ ; these are in good qualitative agreement with the results of Monte Carlo simulations presented in [5, Case 1]. In Fig. 5 (b) we show details of the flow field.

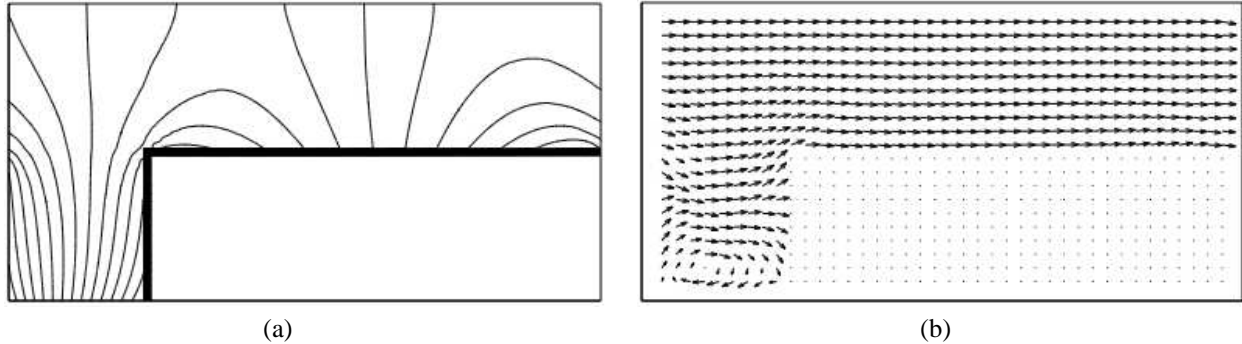


**FIGURE 5.** Knudsen pump, (a) temperature isolines, (b) flow field.

We have also calculated the net flux through the channel depending on the Knudsen number. In agreement with [5] we find the flow growing with the Knudsen number for small values of  $Kn$  and decaying for larger values. In the neighborhood of the maximum, convergence to the steady state is extremely slow. So we used extrapolation techniques for estimates of the fluxes. Therefore we can at present give only qualitative results concerning the relation *Knudsen number versus flow*. Techniques speeding up convergence have for example been presented in [6]. However, these have not yet been implemented for the LGM systems.

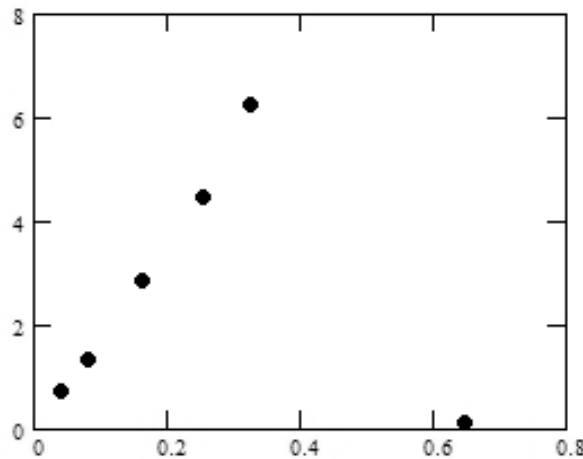


**FIGURE 6.** Knudsen pump, flux vs. Knudsen number.

## BINARY MIXTURES

In a series of numerical experiments we studied an evaporation-condensation problem investigated in [7]. It concerns a binary mixture of two mechanically identical species, one of which (*species A*) interacts with the walls via

condensation and evaporation, while the other one (*species B*) is completely reflected. In [7] it was proven that in the fluid dynamic limit species B forms a boundary layer of macroscopic thickness prohibiting any flow of species A through the wall (a phenomenon termed as “ghost effect”).

For the numerical simulation one has to cope with an extremely low convergence to the steady state for small Knudsen numbers (due to the small flow velocity). Like in the Knudsen pump case we take advantage of extrapolation techniques which are possible in the purely deterministic case. Calculations with the 141 velocity model confirmed the above result. We applied the LGM model to the discrete system of kinetic equations for a gas mixture. Figure 7 (a) shows the boundary layer of species B (solid line) close to the fluid dynamic limit, the density of species A (dashed line) and the sum of both densities (dotted line). Figure 7 (b) displays the mass flow versus the Knudsen number proving the linear decay for  $Kn \rightarrow 0$ .

The above problem can be attacked in an alternative way. A binary system of two mechanically identical species can be modeled with LGM within a single system as we will shortly indicate. Rather than choosing  $\mathcal{V} =: \mathcal{V}_+$  as in formula (1), we could have derived the same model based on

$$\mathcal{V}_- = \{(k, l, m) \in \mathbf{Z}^3 : k + l + m \text{ odd}\} \quad (6)$$

(with the same set  $\mathcal{C}$  of center points). The union  $\mathcal{V}_+ \cup \mathcal{V}_-$  leads to a system with no interaction of velocity pairs in  $\mathcal{V}_+ \times \mathcal{V}_-$ . However, we can extend  $\mathcal{C}$  in such a way that these interactions are possible, e.g. by extending  $\mathcal{C}$  by the set

$$\mathcal{C}_{mix} = \mathbf{Z}^3 + (0.5, 0.5, 0.5)^T.$$

The new system  $(\mathcal{C}_{mix}, \mathcal{V}_+ \cup \mathcal{V}_-)$  has in addition to the physical conservation laws mass, momenta and energy the conservation of

$$\rho_+ = \sum_{k+l+m \text{ even}} f(k, l, m) \quad \text{and} \quad \rho_- = \sum_{k+l+m \text{ odd}} f(k, l, m).$$

Thus the even and odd indices may be used to represent two different interacting species.

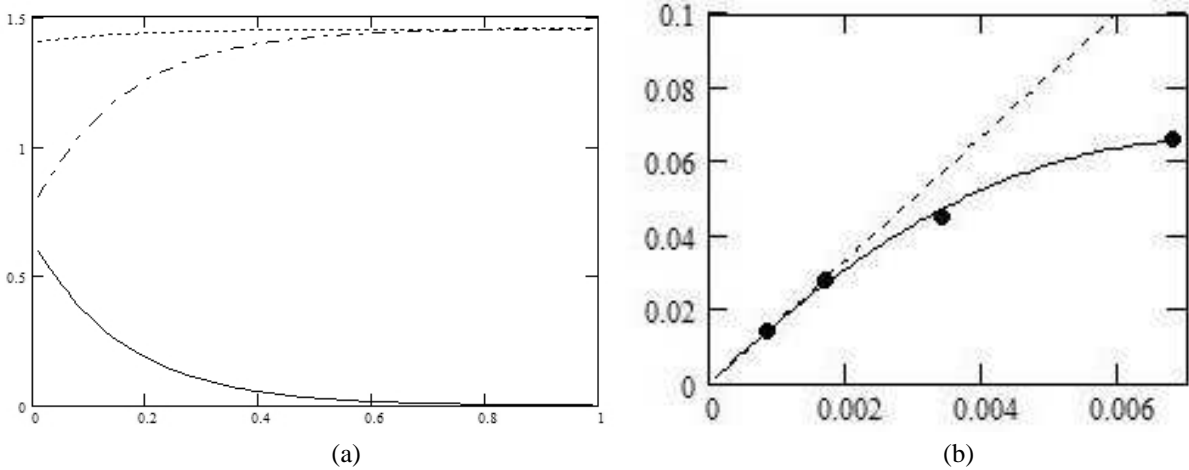


**FIGURE 7.** Evaporation condensation problem, (a) distributions, (b) flow field vs. Knudsen number.

## CONCLUDING REMARKS AND FUTURE PERSPECTIVES

We have demonstrated that LGM’s provide a powerful tool for the numerical simulation of rarefied gas flows – provided one takes into account a few specific features of such systems. E.g., schemes of small or modest size encounter discretization and truncation errors. However, since these models are free of random fluctuations, there is a good chance to eliminate these effects via extrapolation techniques.

As yet the implemented version is preliminary. In particular there is a need for features accelerating the approach to steady state solutions. This will be a task for the near future.

LGM's are not intended to replace well-established numerical simulation tools like Monte Carlo systems. E.g. there is a number of real gas effects which are not easy to implement in LGM's. However, LGM's present an alternative view on rarefied gas flows and may be useful in a number of situations.

We want to point out that a Monte Carlo version of an LGM is readily established by constructing a stochastic collision operator. To this end we replace the inner sum of (3),  $\sum_{o \in \mathcal{O}} \gamma_o f(c+w)f(c-w) \cdot \Phi(c+ow)$  with the term  $\gamma f(c+w)f(c-w) \cdot \Phi(c+o_r w)$  with  $o_r \in \mathcal{O}$  being randomly chosen according to the probability

$$P(o_r) = \gamma_{o_r} / \gamma, \quad \gamma = \sum_{o \in \mathcal{O}} \gamma_o. \quad (7)$$

In the numerical simulation this means that rather than redistributing the pre-collisional amount  $\gamma f(v)f(c-(v-c))$  over the whole discrete ball  $S_{c,v}$ , we pass it over to one single randomly chosen pair, similarly as it is done in DSMC calculations. Let us denote the corresponding random collision operator by  $J^{stoch}[f]$ . An appealing fact is that in our model we can adjust stochasticity to any amount we wish by switching to the convex combination

$$\lambda J^{stoch}[f] + (1-\lambda)J[f], \quad \lambda \in [0, 1]. \quad (8)$$

This enables us to investigate the influence of stochasticity in numerical MC schemes. Furthermore, this model may help to observe the establishment of flow instabilities. First simulation results promise interesting insights into the role of randomness in physical and numerical systems. This will establish a new focus of research for the near future.

## REFERENCES

1. H. Babovsky, "Kinetic models on orthogonal groups and the simulation of the Boltzmann equation" in *Proceedings of 26th International Symposium on Rarefied Gas Dynamics*, edited by T. Abe, AIP Conference Proceedings 1084, Melville, New York, 2009, pp. 415-420.
2. H. Babovsky, *Computers and Mathematics with Applications* **58**, 791-804 (2009).
3. J. H. Conway, and N. J. A. Austin, *Sphere Packings, Lattices and Groups*, Springer, New York, 1999.
4. D. J. Rader, M. A. Gallis, J. R. Torczynski and W. Wagner, *Phys. Fluids* **18**, 077102 (2006).
5. Y. Sone, Y. Waniguchi and K. Aoki, *Phys. Fluids* **8**, 2227-2235 (1996).
6. H. Babovsky, D. Görsch and F. Schilder, "Steady kinetic boundary value problems" in *Lecture Notes on the Discretization of the Boltzmann Equation*, edited by N. Bellomo and R. Gatignol, World Scientific, 2002, pp. 131-156.
7. S. Takata and K. Aoki, *Phys. Fluids* **11**, 2743-2756 (1999).